RESEARCH ARTICLE | APRIL 05 2023

## High conductivity in Ge-doped AIN achieved by a non-equilibrium process *⊙*

Pegah Bagheri ■ ⑩; Cristyan Quiñones-Garcia ⑩; Dolar Khachariya ⑩; James Loveless ⑩; Yan Guan; Shashwat Rathkanthiwar ⑩; Pramod Reddy ⑩; Ronny Kirste ⑩; Seiji Mita; James Tweedie; Ramón Collazo ⑩; Zlatko Sitar ⑩

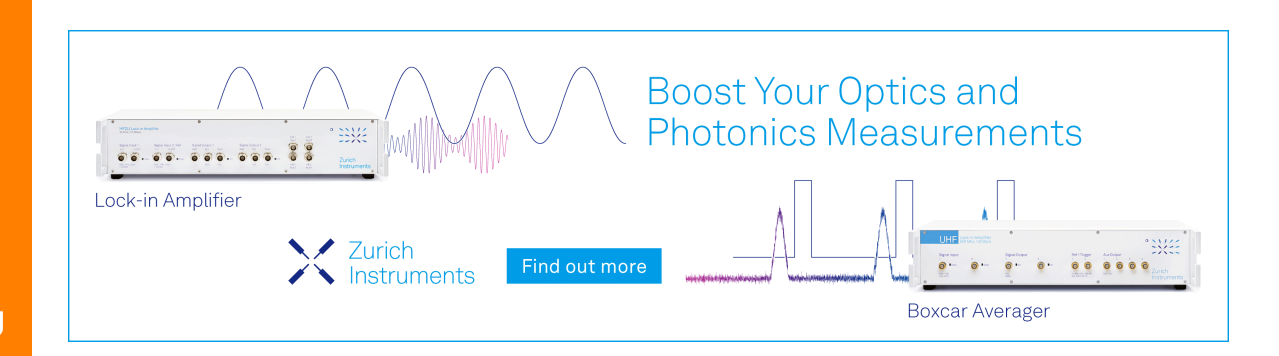


Appl. Phys. Lett. 122, 142108 (2023) https://doi.org/10.1063/5.0146439





CrossMark





# High conductivity in Ge-doped AIN achieved by a non-equilibrium process

Cite as: Appl. Phys. Lett. **122**, 142108 (2023); doi: 10.1063/5.0146439 Submitted: 13 February 2023 · Accepted: 23 March 2023 · Published Online: 5 April 2023







Pegah Bagheri,<sup>1,a)</sup> (D) Cristyan Quiñones-Garcia,<sup>1</sup> (D) Dolar Khachariya,<sup>2</sup> (D) James Loveless,<sup>1</sup> (D) Yan Guan,<sup>1</sup> Shashwat Rathkanthiwar,<sup>1</sup> (D) Pramod Reddy,<sup>2</sup> (D) Ronny Kirste,<sup>2</sup> (D) Seiji Mita,<sup>2</sup> James Tweedie,<sup>2</sup> Ramón Collazo,<sup>1</sup> (D) and Zlatko Sitar<sup>1,2</sup> (D)

### **AFFILIATIONS**

<sup>1</sup>Department of Materials Science and Engineering, North Carolina State University, Raleigh, North Carolina 27695, USA <sup>2</sup>Adroit Materials, Cary, North Carolina 27518, USA

### **ABSTRACT**

Highly conductive Ge-doped AlN with conductivity of 0.3 ( $\Omega$  cm)<sup>-1</sup> and electron concentration of  $2 \times 10^{18}$  cm<sup>-3</sup> was realized via a non-equilibrium process comprising ion implantation and annealing at a moderate thermal budget. Similar to a previously demonstrated shallow donor state in Si-implanted AlN, Ge implantation also showed a shallow donor behavior in AlN with an ionization energy  $\sim$ 80 meV. Ge showed a 3× higher conductivity than its Si counterpart for a similar doping level. Photoluminescence spectroscopy indicated that higher conductivity for Ge-doped AlN was achieved primarily due to lower compensation. This is the highest n-type conductivity reported for AlN doped with Ge to date and demonstration of technologically useful conductivity in Ge-doped AlN.

Published under an exclusive license by AIP Publishing. https://doi.org/10.1063/5.0146439

AlN is an ultrawide bandgap semiconductor (6.1 eV) possessing a high breakdown field (>15 MV/cm) and high thermal conductivity. These intrinsic properties make it a candidate for deep UV optoelectronics (emitting wavelength at 210 nm), high-power and highfrequency applications in which it can readily surpass GaN and SiC and as a host for quantum hardware.  $^{2-4}$  However, controllable n- and p-type doping from  $10^{16}$  to  $10^{20}$  cm $^{-3}$  is necessary to provide high mobility drift layers and highly conductive contact layers, essential for AlN-based electronics and optoelectronics. The transition from shallow donors to deep states and dopant compensation, mainly via carbon, dislocations and VIII-donor complexes, have been identified as the main limitations to controlled n-type doping in AlN. 5-8 Group IV dopants, such as Si and Ge, are expected to occupy the metal sites in AlN (Ge<sub>Al</sub> and Si<sub>Al</sub>), since their substitution on the nitrogen site is associated with a high formation energy. Therefore, both Ge and Si act as donors with an extra electron after substitution on the metal site. In the shallow donor state, the ionization energy of Si and Ge is expected to be around 75 meV depending only on the host properties.<sup>5</sup> However, the transition to a deep state upon relaxation of the donors in Al site is expected to increase the ionization energy. 10,111 The increase in the ionization energy of donors in Al-rich AlGaN and AlN to ~250 meV, resulting in orders of magnitude reduction in the free carrier concentration, was originally attributed to the formation of DX<sup>-1,5,12</sup> DX<sup>-1</sup> is a type of self-compensation that pins the Fermi level at hundreds of meV below the conduction band and, hence, significantly reduces carrier concentration and fundamentally constrains the possibility of doping.<sup>13</sup> However, a recent work by Bagheri et al. provided a direct proof of single electron occupancy for donors in AlGaN and AlN rather than DX formation. <sup>14</sup> Consequently, technologically relevant n-type conductivity in AlN can be achieved via doping with either Si or Ge and simultaneous management of compensating point defects via chemical potential control (CPC) and/ or defect quasi fermi level (dQFL) control methods.<sup>8,15,16</sup> Interestingly, non-equilibrium methods that inhibit donors from transitioning into their equilibrium deep state are alternative pathways to achieve highly conductive AlN. 17-19 It was shown that Si implantation into AlN, followed by a 1200 °C recovery annealing, effectively inhibited Si from forming the stable deep donor state and exhibits low ionization energy ( $\sim$ 75 meV), as predicted for a hydrogenic shallow donor in AlN. <sup>19</sup> It has been hypothesized that the use of non-equilibrium doping methods, such as ion implantation, can limit the formation of the donor equilibrium state (deep donor), by kinetically stabilizing the donor in a metastable state (shallow donor) during a judicious annealing process. By controlling compensation of this donor via above bandgap illumination during the recovery annealing process, an n-type conductivity of  $\sim 3 (\Omega \text{ cm})^{-1}$  and a free electron concentration of  $\sim 5 \times 10^{18} \text{ cm}^{-1}$ 

a) Author to who correspondence should be addressed: pbagher@alumni.ncsu.edu

were achieved in AlN.<sup>18</sup> Ge is another donor candidate in III-Ns, leading to n-type conductivity in AlGaN.<sup>20–23</sup> While Ge showed promise for lower Al molar fractions, where it resulted in higher maximum carrier concentrations than Si due to a relatively high formation energy of  $V_{\rm III}$ -nGe $_{\rm III}$  complexes,<sup>10,21</sup> it transitioned to a deep donor state at lower Al content than Si (0.5 vs 0.8 Al content), resulting in highly resistive Al-rich AlGaN.<sup>13,24</sup> Similar to Si, it is expected that the transition of Ge to a deep donor may be prevented by the use of a non-equilibrium doping process, thus enabling n-doping of AlN by Ge.

In this work, we demonstrated highly conductive Ge-doped AlN via a non-equilibrium doping process, which supports our hypothesis that by non-equilibrium doping methods, the metastable dopant state can be kinetically stabilized, leading to the control of the dopant distribution between the shallow and deep states. Having demonstrated this for both Ge- and Si-doped AlN supports the universality of this hypothesis.

AlN homoepitaxial films were grown on AlN single crystal substrates (dislocation density < 10<sup>3</sup> cm<sup>-3</sup>) in a vertical, low-pressure (20 Torr), RF-heated, cold-walled MOCVD reactor. Trimethylaluminum (TMA) and ammonia were used as aluminum and nitrogen precursors, respectively. Details on epitaxial growth on AlN substrates and its surface preparation are explained somewhere else.  $^{25-27}$  A 2  $\mu$ m thick AlN (V/III = 500), followed by a 500 nm thick unintentionally doped (UID) AlN (V/III = 1000) at 1100 °C, was grown with the intention of minimizing the  $C_N$  concentration ( $<5 \times 10^{17}$  cm<sup>-3</sup>) in the film with a higher V/III ratio. Si and Ge were implanted at room temperature into the top UID AlN film, following a typical single step implantation (Gaussian) profile. The implanted species (Si and Ge) are different in terms of mass and ionic radius. While Si is smaller with about 26 pm as ionic radius, Ge (39 pm) is larger than Si and as large as Al.<sup>28</sup> Therefore, the dose and energy were calculated accordingly to achieve similar implantation profile for both species. Table I describes the implantation conditions. A tilt angle of 7° was used to reduce ion channeling during implantation.

Post-implantation annealing for damage recovery was realized under a  $N_2$  ambient at a pressure of 100 Torr for 120 min at a temperature of 1200 °C. Further details on the optimal annealing conditions are discussed elsewhere. As reported previously, the change in the implantation profile by annealing with low thermal budget is negligible. Therefore, the depth profiles for both dopants are expected to remain similar to the implantation profile after annealing at 1200 °C for 120 min. Both Ge- and Si-doped AlN films showed smooth surface morphology with bilayer step structure with RMS roughness <1 nm, as observed by atomic force microscopy before and after implantation and annealing. Damage recovery after post-implantation annealing was investigated by high-resolution x-ray diffraction (XRD) measurements using a Philips X'Pert materials research diffractometer with a Cu anode. Electrical characterization was performed using temperature-dependent Hall measurements (8400 series Lakeshore

TABLE I. Si and Ge implantation conditions in AIN.

Species	Energy (keV)	Dose (cm <sup>-2</sup> )	Peak concentration (cm <sup>-3</sup> )	Projected range (nm)
Si Ge	100 210	10 <sup>14</sup> 10 <sup>14</sup>	$\sim 10^{19} \\ \sim 10^{19}$	100 100

AC/DC Hall system) in the van der Pauw configuration from RT to 700 K. The contacts  $(2 \times 2 \text{ mm}^2)$  were patterned at the corners of 1 × 1 cm<sup>2</sup> samples. Prior to the measurement, a contact stack consisting of V/Al/Ni/Au (30/100/70/70 nm) was deposited onto the etched surface by electron beam evaporation. Contacts were annealed at 850 °C for 1 min via rapid thermal annealing. Details on the surface etching and contacts preparation were explained somewhere else. 19 The Hall measurements were performed in the current ranges  $\sim 10 \ \mu A$  (voltage  $> 20 \ V$ ) where the contacts exhibited an Ohmic behavior. The resistivity values were measured at three different currents in the Ohmic regime (voltage > 20 V) yielding similar results (variation < 5%). Photoluminescence (PL) spectroscopy using a 193 nm ArF excimer laser was implemented to identify and track point defect formation resulting from the implantation and annealing processes. A Princeton Instruments Acton SP2750 0.75 m highresolution monochromator, with a 3200 grooves/mm optical grating, and a PIXIS: 2KBUV Peltier-cooled charge-coupled device camera were used to acquire the PL spectra at room temperature.

Figure 1 shows symmetric  $2\theta-\omega$  scans for as-implanted and annealed AlN after Si and Ge implantation. Additional, strain-related peaks were observed at lower angles from the Bragg peak. These peaks are characteristics signature of damage after implantation. As-implanted AlN was electrically resistive and optically dead (no luminescence was detected via PL). As such, post-implantation annealing was essential to recover crystallinity and electrical and optical properties. Following the procedure described in a previous publication by Breckenridge *et al.*, the Ge- and Si-implanted AlN was annealed at 1200 °C for 120 min. This was sufficient to recover the AlN crystallinity and to observe the shallow donor behavior for Si. Figure 1(b) shows the  $2\theta-\omega$  scans after annealing for 120 min at 1200 °C. Full recovery was observed for both Ge- and Si-doped samples, as evidenced by the disappearance of strain-related peaks.

Following the recovery of structural properties, electrical and optical properties of Si- and Ge-implanted AlN were investigated. Interestingly, after implantation and annealing at 1200 °C for 120 min, both Si and Ge showed n-type conductivity of 0.1 and 0.3  $(\Omega \text{ cm})^{-1}$  at room temperature, respectively. This n-type conductivity in implanted and annealed AlN is more than one order of magnitude higher than the values reported for Si doping during epitaxy.<sup>8</sup> It is worth mentioning that Ge-doped AlN by epitaxy results in highly resistive films with no room temperature conductivity, as Ge transitions to the deep donor state already at 50% Al in AlGaN. 14,24 This work shows that following a non-equilibrium process consisting of ion implantation and relatively low thermal budget annealing,<sup>32</sup> n-type conductivity via Ge doping in AlN can be achieved and results in a 3× higher conductivity than that observed in Si-implanted and annealed films. Figure 2 shows temperature-dependent conductivity measurements performed on films with different implantation species. Both Ge and Si exhibit a shallow donor behavior with an ionization energy of  $80 \pm 10$  meV, as extracted from temperature dependence of conductivity. Donor concentration (N<sub>d</sub>) was considered to be 10<sup>19</sup> cm<sup>-3</sup> for both Si- and Gedoped AlN (as intended for the implantation) in the charge balance model. Details on the charge balance model for conductivity and the fitting parameters in n-type AlN can be found elsewhere. 18 The observation of the shallow donor ionization energy for both donors supports the main hypothesis that by non-equilibrium doping methods the metastable shallow dopant state can be kinetically stabilized. Both donor species should have the same ionization energy in their

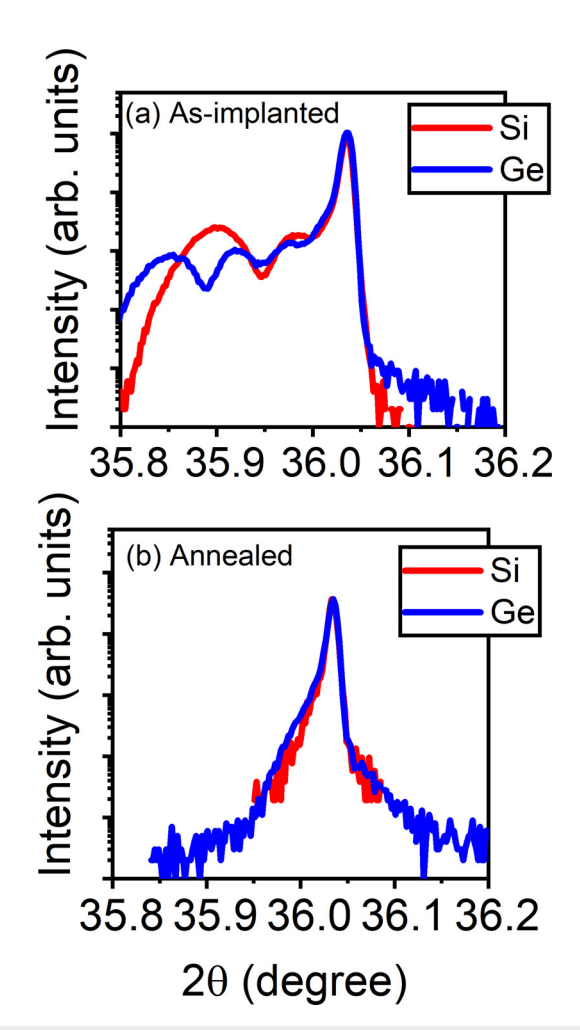


**FIG. 1.** High-resolution x-ray diffraction  $2\theta$ – $\omega$  scans for Si- and Ge-implanted AIN: (a) as-implanted and (b) annealed. Strain-related peaks vanished after a 1200 °C anneal for 120 min, signifying damage recovery.

hydrogenic shallow state as it depends only on the semiconductor matrix (dielectric constant and effective mass). Temperaturedependent Hall measurements were also performed on the Geimplanted AlN. As shown in Fig. 3, the carrier concentration at room temperature was  $>10^{18}$  cm<sup>-3</sup> (sheet concentration of 3  $\times$  10<sup>13</sup> cm<sup>-2</sup>) while it saturated at low-10<sup>19</sup> cm<sup>-3</sup> (sheet concentration of low-10<sup>14</sup> cm<sup>-2</sup>) at higher temperatures, corresponding to full donor ionization. The room temperature mobility was  $\sim 0.4 \,\mathrm{cm^2/V}$  s; the mobility was expected to be low due to the high ionized impurity scattering at high (shallow) dopant concentrations, formation of point defects during implantation, and Gaussian depth profile of the dopants in the conductive layer. 8,19 The ionization energy of Ge in AlN was estimated to be  $\sim$ 90  $\pm$  20 meV based on charge balance fitting to Fig. 3(a) which is in agreement with Fig. 2. It is worth noting that, for n-type AlN, the charge balance model to extract compensation ratio is valid only when the doping range does not favor the formation of VAI-nGeAI complexes. In the self-compensation regime, Ge not only incorporates in the donor state but also forms the complexes and, therefore, [Ge]total

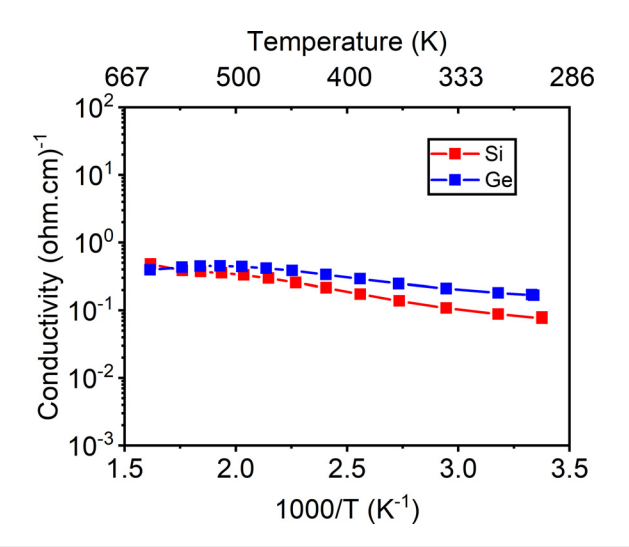


**FIG. 2.** Temperature-dependent conductivity of Si- and Ge-implanted AIN after annealing for 120 min at 1200  $^{\circ}$ C. Solid lines between the data points serve as the guide to the eye.

 $\neq$  [Ge]<sub>donor</sub>. However, as shown in Fig. 3(a), the carrier concentration at high temperature saturated close to the intended Ge concentration, suggesting a low compensation ratio.

To further understand the differences between Si and Ge doping, RT PL measurements were performed as shown in Fig. 4. Defect luminescence at around 3 eV (400 nm) in AlN has been identified as V<sub>III</sub>-nSi<sub>III</sub>/Ge<sub>III</sub> complexes. Strong luminescence at 400 nm observed on Si-implanted AlN suggests the significant presence of V<sub>III</sub>-nSi<sub>III</sub>-related complexes. No luminescence at 400 nm was observed for Ge-implanted AlN. As determined for AlGaN, Ge-related complexes have a higher formation energy than their Si counterparts. Moreover, Ge doping showed a very different "knee behavior" than Si, corresponding to a different stability of the various charged complex states as a function of Ge concentration. 10,21 As such, two factors contributed to the 3× higher n-type conductivity for Ge-doped AlN: (1) Ge in the shallow donor state and (2) low concentration of compensating Ge-related complexes. Washiyama et al. observed 2X-3X higher maximum electron concentration at RT for Ge-doped Al<sub>0.3</sub>Ga<sub>0.7</sub>N, as compared to Si-doped Al<sub>0.3</sub>Ga<sub>0.7</sub>N, which is in agreement with our observations in AlN.<sup>21</sup> It is worth noting that the peak at 460 nm (2.7 eV) in AlN is suggested to be related to a charged configuration of V<sub>Al</sub> by previous DFT models. 11,34 These metal vacancies are likely to be generated in non-equilibrium concentrations during implantation. A low thermal budget annealing (1200 °C) might not be sufficient to eliminate these vacancies,<sup>35</sup> as suggested by the PL results in Fig. 4. Following our previous observations, <sup>18</sup> the intensity of the 2.7 eV peak can be reduced significantly using dQFL control. This suggests that the incorporated metal vacancies are, indeed, in a charged configuration, supporting the assignment previously discussed.

This report is not only the demonstration of n-type conductivity in Ge-doped AlN but also the demonstration of the Ge shallow donor state, resulting in technologically relevant conductivity in AlN. This work further supports the predicted universality of using ion implantation coupled with low thermal budget recovery annealing and dopant

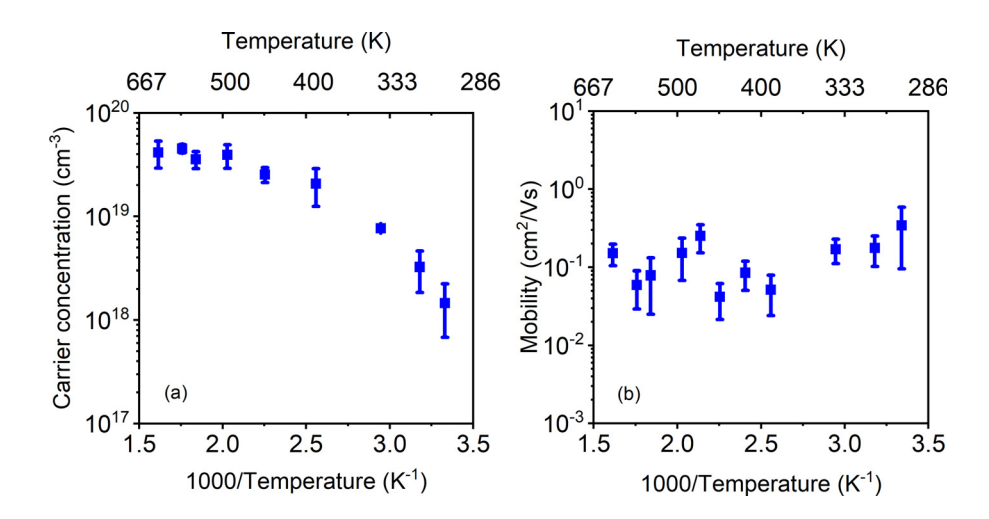
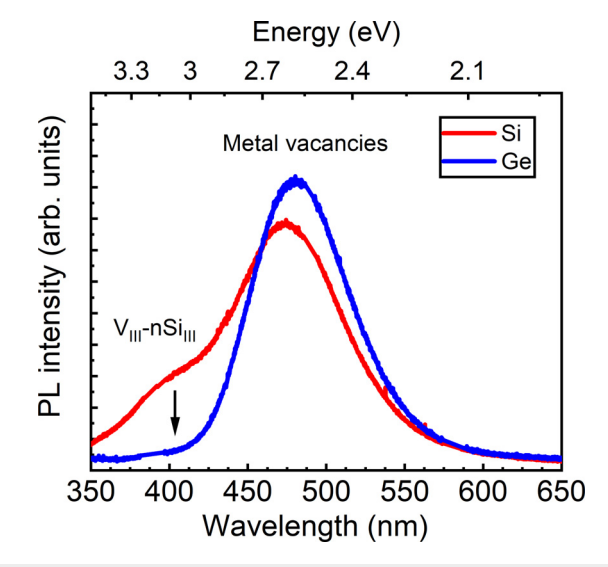


FIG. 3. Temperature-dependent (a) carrier concentration and (b) mobility for Ge-implanted AIN after annealing at 1200 °C for 120 min. Error bars indicate the experimental error obtained by multiple measurements.

activation as a non-equilibrium doping method to achieve metastable shallow donor states in AlN, enabling high n-type conductivity. This approach could be expanded to other wide or ultrawide bandgap semiconductors, where the stable or most likely state for its dopants is a deep state. As the shallow donor state is kinetically stabilized, the annealing conditions as generalized in terms of thermal budget (temperature and time) are important for the selection between the shallow and deep donor states. As such, mapping of the energy-landscape of these states to characterize the parameters that determine their occupancy will provide information on the robustness of this doping process. In general, the implementation of CPC and dQFL methods to minimize point defects along with Ge implantation offers a possible pathway to not only further reduce compensation but also to obtaining a shallow donor behavior that would result in higher n-type conductivity and mobility in AlN.<sup>18,29</sup>



**FIG. 4.** RT PL spectra for Si- and Ge-implanted AlN after annealing at 1200 °C for 120 min. While n-type conductivity and shallow donor behavior were observed for Si- and Ge-implanted AlN, the latter samples showed much lower compensation.

In this work, the electrical and optical properties of Si- and Geimplanted AlN were investigated. Both dopants showed a shallow donor behavior with an ionization energy of  ${\sim}80\,\text{meV}$  and high n-type conductivity at room temperature. Ge showed  $3\times$  higher conductivity than its Si counterpart with electron concentration as high as  $2\times10^{18}\,\text{cm}^{-3}$ . PL indicated that this was primarily due to a lower compensation in Ge-doped samples, which arose as a result of higher formation energy of  $V_{\rm III}$ –nGe $_{\rm III}$  complexes as compared their Si counterparts. This demonstrates that Ge is a technologically viable dopant in AlN if it is kinetically stabilized in the metastable shallow donor states via a non-equilibrium doping process. The same method could be expanded to other wide or ultrawide bandgap semiconductors, where the stable or most likely state for its dopants is a deep state, to achieve useful doping.

The authors gratefully acknowledge funding in part from AFOSR (Nos. FA9550-17-1-0225 and FA9550-19-1-0114), DoD ARPA-E (No. DE-AR0001493), NSF (Nos. ECCS-1508854, ECCS-1916800, and ECCS-1653383), and Army Research Office (ARO) (W911NF-22-20171).

### AUTHOR DECLARATIONS Conflict of Interest

The authors have no conflicts to disclose.

### **Author Contributions**

Pegah Bagheri: Conceptualization (lead); Data curation (lead); Formal analysis (lead); Investigation (equal); Methodology (lead); Project administration (equal); Software (lead); Supervision (equal); Validation (equal); Visualization (equal); Writing – original draft (lead); Writing – review & editing (equal). James Tweedie: Conceptualization (equal); Investigation (equal); Project administration (equal); Validation (equal); Visualization (equal); Writing – review & editing (equal). Ramon Collazo: Conceptualization (equal); Formal analysis (equal); Funding acquisition (lead); Investigation (lead); Project administration (lead); Resources (lead); Supervision (lead); Validation (equal); Visualization (equal); Writing – review &

editing (lead). Zlatko Sitar: Conceptualization (equal); Funding acquisition (lead); Investigation (equal); Project administration (lead); Resources (lead); Supervision (lead); Validation (equal); Visualization (equal); Writing - review & editing (lead). Cristyan Quinones-Garcia: Data curation (equal); Investigation (equal); Methodology (equal). Dolar Khachariya: Data curation (equal); Methodology (equal). James Terrell Loveless: Data curation (equal); Formal analysis (supporting); Methodology (equal). Yan Guan: Data curation (equal); Formal analysis (supporting); Methodology (equal). Shashwat Rathkanthiwar: Conceptualization (supporting); Formal analysis (supporting); Methodology (equal); Validation (supporting); Visualization (supporting). Pramod Reddy: Conceptualization (equal); Formal analysis (equal); Investigation (equal); Supervision (equal); Validation (equal); Visualization (equal); Writing - review & editing (equal). Ronny Kirste: Conceptualization (equal); Supervision (equal); Validation (equal); Visualization (equal); Writing - review & editing (equal). Seiji Mita: Conceptualization (equal); Data curation (equal); Methodology (equal); Supervision (equal); Validation (equal); Visualization (equal).

### **DATA AVAILABILITY**

The data that support the findings of this study are available within the article.

### REFERENCES

- <sup>1</sup>J. Y. Tsao, S. Chowdhury, M. A. Hollis, D. Jena, N. M. Johnson, K. A. Jones, R. J. Kaplar, S. Rajan, C. G. V. de Walle, E. Bellotti, C. L. Chua, R. Collazo, M. E. Coltrin, J. A. Cooper, K. R. Evans, S. Graham, T. A. Grotjohn, E. R. Heller, M. Higashiwaki, M. S. Islam, P. W. Juodawlkis, M. A. Khan, A. D. Koehler, J. H. Leach, U. K. Mishra, R. J. Nemanich, R. C. N. Pilawa-Podgurski, J. B. Shealy, Z. Sitar, M. J. Tadjer, A. F. Witulski, M. Wraback, and J. A. Simmons, "Ultrawide-bandgap semiconductors: Research opportunities and challenges," Adv. Electron. Mater. 4(1), 1600501 (2018).
- <sup>2</sup>Y. Taniyasu, M. Kasu, and T. Makimoto, "An aluminium nitride light-emitting diode with a wavelength of 210 nanometres," Nature 441(7091), 325–328 (2006).
- <sup>3</sup>T. Kinoshita, T. Nagashima, T. Obata, S. Takashima, R. Yamamoto, R. Togashi, Y. Kumagai, R. Schlesser, R. Collazo, A. Koukitu, and Z. Sitar, "Fabrication of vertical Schottky barrier diodes on n-type freestanding AlN substrates grown by hydride vapor phase epitaxy," Appl. Phys. Express 8(6), 061003 (2015)
- <sup>4</sup>J. B. Varley, A. Janotti, and C. G. Van de Walle, "Defects in AlN as candidates for solid-state qubits," Phys. Rev. B **93**(16), 161201 (2016).
- <sup>5</sup>R. Collazo, S. Mita, J. Xie, A. Rice, J. Tweedie, R. Dalmau, and Z. Sitar, "Progress on n-type doping of AlGaN alloys on AlN single crystal substrates for UV opto-electronic applications," Phys. Status Solidi C 8(7–8), 2031–2033 (2011).
- <sup>6</sup>I. Bryan, Z. Bryan, S. Washiyama, P. Reddy, B. Gaddy, B. Sarkar, M. H. Breckenridge, Q. Guo, M. Bobea, J. Tweedie, S. Mita, D. Irving, R. Collazo, and Z. Sitar, "Doping and compensation in Al-rich AlGaN grown on single crystal AlN and sapphire by MOCVD," Appl. Phys. Lett. 112(6), 062102 (2018).
- <sup>7</sup>F. Kaess, S. Mita, J. Xie, P. Reddy, A. Klump, L. H. Hernandez-Balderrama, S. Washiyama, A. Franke, R. Kirste, A. Hoffmann, R. Collazo, and Z. Sitar, "Correlation between mobility collapse and carbon impurities in Si-doped GaN grown by low pressure metalorganic chemical vapor deposition," J. Appl. Phys. 120(10), 105701 (2016).
- <sup>8</sup>P. Bagheri, C. Quiñones-Garcia, D. Khachariya, S. Rathkanthiwar, P. Reddy, R. Kirste, S. Mita, J. Tweedie, R. Collazo, and Z. Sitar, "High electron mobility in AlN:Si by point and extended defect management," J. Appl. Phys. 132(18), 185703 (2022).
- <sup>9</sup>C. G. Van de Walle and J. Neugebauer, "First-principles calculations for defects and impurities: Applications to III-nitrides," J. Appl. Phys. 95(8), 3851–3879 (2004).

- <sup>10</sup>J. N. Baker, P. C. Bowes, J. S. Harris, R. Collazo, Z. Sitar, and D. L. Irving, "Complexes and compensation in degenerately donor doped GaN," Appl. Phys. Lett. 117(10), 102109 (2020).
- <sup>11</sup>J. S. Harris, J. N. Baker, B. E. Gaddy, I. Bryan, Z. Bryan, K. J. Mirrielees, P. Reddy, R. Collazo, Z. Sitar, and D. L. Irving, "On compensation in Si-doped AlN," Appl. Phys. Lett. 112(15), 152101 (2018).
- <sup>12</sup>R. Zeisel, M. W. Bayerl, S. T. B. Goennenwein, R. Dimitrov, O. Ambacher, M. S. Brandt, and M. Stutzmann, "DX-behavior of Si in AlN," Phys. Rev. B 61(24), R16283(R) (2000)
- <sup>13</sup>L. Gordon, J. L. Lyons, A. Janotti, and C. G. Van de Walle, "Hybrid functional calculations of DX centers in AlN and GaN," Phys. Rev. B 89(8), 085204 (2014).
- <sup>14</sup>P. Bagheri, P. Reddy, S. Mita, D. Szymanski, J. H. Kim, Y. Guan, D. Khachariya, A. Klump, S. Pavlidis, R. Kirste, R. Collazo, and Z. Sitar, "On the Ge shallow-to-deep level transition in Al-rich AlGaN," J. Appl. Phys. 130(5), 055702 (2021).
- <sup>15</sup>P. Reddy, S. Washiyama, F. Kaess, R. Kirste, S. Mita, R. Collazo, and Z. Sitar, "Point defect reduction in MOCVD (Al)GaN by chemical potential control and a comprehensive model of C incorporation in GaN," J. Appl. Phys. 122(24), 245702 (2017).
- <sup>16</sup>P. Reddy, M. P. Hoffmann, F. Kaess, Z. Bryan, I. Bryan, M. Bobea, A. Klump, J. Tweedie, R. Kirste, S. Mita, M. Gerhold, R. Collazo, and Z. Sitar, "Point defect reduction in wide bandgap semiconductors by defect quasi Fermi level control," J. Appl. Phys. 120(18), 185704 (2016).
- <sup>17</sup>S. Washiyama, P. Reddy, B. Sarkar, M. H. Breckenridge, Q. Guo, P. Bagheri, A. Klump, R. Kirste, J. Tweedie, S. Mita, Z. Sitar, and R. Collazo, "The role of chemical potential in compensation control in Si:AlGaN," J. Appl. Phys. 127(10), 105702 (2020).
- <sup>18</sup>M. H. Breckenridge, P. Bagheri, Q. Guo, B. Sarkar, D. Khachariya, S. Pavlidis, J. Tweedie, R. Kirste, S. Mita, P. Reddy, R. Collazo, and Z. Sitar, "High n-type conductivity and carrier concentration in Si-implanted homoepitaxial AlN," Appl. Phys. Lett. 118(11), 112104 (2021).
- <sup>19</sup>M. Hayden Breckenridge, Q. Guo, A. Klump, B. Sarkar, Y. Guan, J. Tweedie, R. Kirste, S. Mita, P. Reddy, R. Collazo, and Z. Sitar, "Shallow Si donor in ion-implanted homoepitaxial AlN," Appl. Phys. Lett. 116(17), 172103 (2020).
- 20P. Bagheri, J. H. Kim, S. Washiyama, P. Reddy, A. Klump, R. Kirste, S. Mita, R. Collazo, and Z. Sitar, "A pathway to highly conducting Ge-doped AlGaN," J. Appl. Phys. 130(20), 205703 (2021).
- <sup>21</sup>S. Washiyama, K. J. Mirrielees, P. Bagheri, J. N. Baker, J.-H. Kim, Q. Guo, R. Kirste, Y. Guan, M. H. Breckenridge, A. J. Klump, P. Reddy, S. Mita, D. L. Irving, R. Collazo, and Z. Sitar, "Self-compensation in heavily Ge doped AlGaN: A comparison to Si doping," Appl. Phys. Lett. 118(4), 042102 (2021).
- <sup>22</sup>A. Bansal, K. Wang, J. S. Lundh, S. Choi, and J. M. Redwing, "Effect of Ge doping on growth stress and conductivity in Al<sub>x</sub>Ga<sub>1-x</sub>N," Appl. Phys. Lett. 114(14), 142101 (2019).
- 23 R. Kirste, M. P. Hoffmann, E. Sachet, M. Bobea, Z. Bryan, I. Bryan, C. Nenstiel, A. Hoffmann, J.-P. Maria, R. Collazo, and Z. Sitar, "Ge doped GaN with controllable high carrier concentration for plasmonic applications," Appl. Phys. Lett. 103(24), 242107 (2013).
- <sup>24</sup>P. Bagheri, R. Kirste, P. Reddy, S. Washiyama, S. Mita, B. Sarkar, R. Collazo, and Z. Sitar, "The nature of the DX state in Ge-doped AlGaN," Appl. Phys. Lett. 116(22), 222102 (2020).
- <sup>25</sup>A. Rice, R. Collazo, J. Tweedie, R. Dalmau, S. Mita, J. Xie, and Z. Sitar, "Surface preparation and homoepitaxial deposition of AlN on (0001)-oriented AlN substrates by metalorganic chemical vapor deposition," J. Appl. Phys. 108(4), 043510 (2010).
- <sup>26</sup>R. Dalmau, B. Moody, R. Schlesser, S. Mita, J. Xie, M. Feneberg, B. Neuschl, K. Thonke, R. Collazo, A. Rice, J. Tweedie, and Z. Sitar, "Growth and characterization of AlN and AlGaN epitaxial films on AlN single crystal substrates," J. Electrochem. Soc. 158(5), H530 (2011).
- <sup>27</sup>I. Bryan, A. Rice, L. Hussey, Z. Bryan, M. Bobea, S. Mita, J. Xie, R. Kirste, R. Collazo, and Z. Sitar, "Strain relaxation by pitting in AlN thin films deposited by metalorganic chemical vapor deposition," Appl. Phys. Lett. 102(6), 061602 (2013).
- <sup>28</sup>R. D. Shannon, "Revised effective ionic radii and systematic studies of interatomic distances in halides and chalcogenides," Acta Crystallogr. A 32(5), 751–767 (1976).

- 29H. Okumura, S. Suihkonen, J. Lemettinen, A. Uedono, Y. Zhang, D. Piedra, and T. Palacios, "AlN metal-semiconductor field-effect transistors using Si-ion implantation," Jpn. J. Appl. Phys., Part 1 57(4S), 04FR11 (2018).
- <sup>30</sup>C. Ventosa-Moulet, S. Hayashi, and M. S. Goorsky, "Lattice strain and strain evolution in hydrogen-implanted materials: The roles of mechanical properties and hydrogen diffusion," ECS Trans. 33(4), 249–254 (2010).
- <sup>31</sup>U. Dadwal, R. Scholz, P. Kumar, D. Kanjilal, S. Christiansen, U. Gösele, and R. Singh, "Hydrogen implantation-induced large area exfoliation in AlN epitaxial layers," Phys. Status Solidi A 207(1), 29–32 (2010).
- <sup>32</sup>M. H. Breckenridge, J. Tweedie, P. Reddy, Y. Guan, P. Bagheri, D. Szymanski, S. Mita, K. Sierakowski, M. Boćkowski, R. Collazo, and Z. Sitar, "High Mg
- activation in implanted GaN by high temperature and ultrahigh pressure annealing," Appl. Phys. Lett. 118(2), 022101 (2021).
- 33J. Hyun Kim, P. Bagheri, R. Kirste, P. Reddy, R. Collazo, and Z. Sitar, "Tracking of point defects in the full compositional range of AlGaN via photoluminescence spectroscopy," Phys. Status Solidi A 2022, 2200390.
- <sup>34</sup>Q. Yan, A. Janotti, M. Scheffler, and C. G. Van de Walle, "Origins of optical absorption and emission lines in AlN," Appl. Phys. Lett. 105(11), 111104 (2014).
- 35H. Okumura and A. Uedono, "Mg implantation in AlN layers on sapphire substrates," Jpn. J. Appl. Phys., Part 1 62(2), 020901 (2023).